

The effect of oxygen vacancy on structures and optical properties of the lead-free $\text{Ba}_{0.5}\text{Sr}_{0.5}\text{TiO}_3$ by first-principles calculation

Hanjiang Xiu¹, Wenlong Yang¹, Jiaqi Lin^{1,*}, Junsheng Han¹, Yu wang¹,
Li Wang¹, Landi Li¹, Haidong Li¹, Hongguo Sun²

¹ Institute of Application Science, Harbin University of Science and Technology, Harbin, Heilongjiang 150080, China

² Polymer Composites Engineering Laboratory, Changchun Institute of Applied Chemistry, Chinese Academy of Sciences, Changchun, Jilin 130022, China

Email: ljqi405@163.com

Keyword: Barium strontium titanate (BST), O vacancy, optical properties, first-principles

Abstract. The structural and optical properties of lead-free Barium strontium titanate $\text{Ba}_{0.5}\text{Sr}_{0.5}\text{TiO}_3$ with oxygen vacancies (BST-O) were investigated by first-principles calculations of density functional theory. The results show that the O vacancy has significant influence on the electronic structure and optical performance of the materials. The structures generate a phase transition from cubic to tetragonal phase, when an O atom has removed from the pure $\text{Ba}_{0.5}\text{Sr}_{0.5}\text{TiO}_3$ (BST). The electron density conformation is distributed, which induce conspicuous distortion of the oxygen octahedron. The calculated optical properties, complex dielectric function, refractive index, absorption coefficient, show that the absorption spectra of the BST-O have multimodality and smaller amplitude by comparing with ideal BST. And the oxygen vacancy lead the increase of refractive index and the decrease of absorption coefficient in visible light frequency region (1.59~3.11 eV), the optical anisotropism is also found in the BST-O.

Introduction

Barium strontium titanate is one of the well known perovskite materials with its excellent ferroelectric and dielectric performance, which is considered as a candidate to replace lead based materials due to the environment issue. Its desirable high dielectric constant, low dielectric losses, strong remnant polarization and low current leakage has been attractive for its fundamental research, and the material could be used for various applications such as dynamic random, access memory, ceramic capacitors, pyroelectric sensors, infrared detectors, chemical sensor, biosensor, microwave devices and optoelectronic applications in recent years^[1-3].

With the intensive study on BST material, a large quantity of tentative exploration on ceramic, film, composite and doping vario-property of BST have been completed^[4-6]. However, most of the experiments of BST focused on the properties in electrical and microwave frequency^[7]. The optical response of BST is not very clear. The first principle method is an effective and efficient method for material research, which is applied to the study of perovskite type materials in the last decades^[8]. Many typical perovskite materials were studied by this method, such as tantalum niobate (KTN), strontium titanate (SrTiO_3) and lead zirconate titanate (PZT)^[9-11], which has succeed in predicting electronic properties, band structure and optical properties of perovskite materials. The related properties of ideal BST are also investigated though first principle method, but defect state of BST is scarcely researched^[12, 13]. As is well known, the oxygen defects are unavoidable during experimental process, F. M. Pontes et al verified that the postannealing temperature and oxygen atmosphere have important influence on the dielectric properties of BST^[14].

In this paper, the possible defects in the process of the experiment were considered. The two models of the ideal bulk of BST and BST with O vacancy were designed and the effect of oxygen vacancy on structures and optical properties of the lead-free $\text{Ba}_{0.5}\text{Sr}_{0.5}\text{TiO}_3$ were investigated by first-principles in detail.

Calculation details

The structures and optical properties of the lead-free oxygen vacancy $\text{Ba}_{0.5}\text{Sr}_{0.5}\text{TiO}_3$ were calculated by a widely used plane-wave pseudopotential total energy program CASTEP^[15] in the framework DFT. The local density approximation (LDA-CAPZ) is used to describe the electronic-correlation function, which have be seen as a typical and accurate mode for the perovskite materials^[16, 17]. The Broyden–Fletcher–Goldfarb–Shannon (BFGS) algorithm and Vanderbilt-type ultrasoft pseudopotential (USP) were utilized for geometry optimization. In geometry optimization and optical properties computing, the energy cutoff was set as 380 eV and a $3 \times 3 \times 3$ k-point Monkhorst-Park mesh in the Brillouin zone was used. All atoms were not fixed and were relaxed until the total energy variation of each atom was below 5.0×10^{-6} eV/atom and the displacement of each atom was below 5.0×10^{-4} Å. Ba (5s2, 5p6, 6s2), Sr (4s2, 4p6, 5s2), Ti (3s2, 3p6, 3d2, 4s2) and O (2s2, 2p4) were considered as valence electrons configurations. The number of k-point and the cut-off energy were tested by the plane wave energy convergence.

The cubic phase $\text{Ba}_{0.5}\text{Sr}_{0.5}\text{TiO}_3$ is a structure with the space group of PM-3M. The experimental lattice parameter of BST is $a=b=c=3.930$ Å^[18], so empirical value 4.0 Å is chosen as a initial lattice length. A $2 \times 2 \times 2$ supercell of pure BST and a $2 \times 2 \times 2$ supercell of BST with oxygen vacancy were designed as computational models, respectively, which were showed in Fig. 1. The calculations of electronic structure and optical properties were based on the previously optimized models.

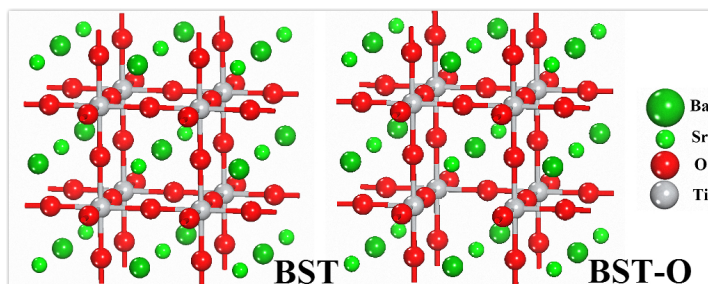


Fig. 1 Supercells of pure BST and BST with oxygen vacancy

Geometry and electrons structures of the BST-O

The structure properties of materials are very important and fundamental for practical applications. In our calculations, the stable ground states of pure BST and BST-O were found after geometry optimization. Computational structure parameters are presented in Table 1. The lattice parameters of pure BST are $a=b=c=7.8036$ Å, $\alpha=\beta=\gamma=90^\circ$ and the cell volume is 475.217 Å³, which is consistent with the experimental data and testifies the structure is classified as cubic phase, PM-3M group^[18]. In contrast, when an O atom point defect is introduced into the system, the lattice parameters are $a=7.8202$ Å, $b=7.8107$ Å, $c=7.8101$ Å and the volume of BST-O is 477.053 Å³. The whole calculated lattice parameters almost approach to experimental values (error less than 1%). From these data, the phase structure of BST-O belong to tetragonal phase which is different from that of BST. The BST-O's cell volume is slight larger than that of pure BST, which suggests that O defect lead to the structure distortion of BST and this result is also in accordance with the previous experiment^[19]. Surprisingly, the comparison of bulk modulus for pure BST and BST-O calculated by LDA indicates the pure BST's bulk modulus is much larger than the BST-O's, from the Table 1, the difference between two models' bulk modulus is 155.49798 GPa, therefore it can be inferred that O vacancy play an important role on mechanical character of BST.

Table 1 Structural parameters, bulk modulus, total energies of pure BST and BST with oxygen vacancy

	BST	BST-O
(a, b, c)	(7.8036 Å, 7.8036 Å, 7.8036 Å)	(7.8202 Å, 7.8107 Å, 7.8101 Å)
(α, β, γ)	(90.000°, 90.000°, 90.000°)	(89.872°, 90.000°, 90.000°)
$V(\text{Å}^3)$	475.217	477.053
$B(\text{GPa})$	361.47364	205.97566
$E_{\text{total}}(\text{eV})$	-29539.26959	-29099.45364

In terms of the energy of BST, there is an ascending trend when an O atom is removed. Calculated by Eq. (1) in which 0 or 1 is selected as the numerical value of x , the value of the formation enthalpy of BST and BST-O are -43.34 eV and -41.95 eV, these results certify that the pure BST and the BST with oxygen vacancy is thermodynamically stable.

$$\Delta H_f [Ba_{0.5}Sr_{0.5}TiO_{(24-x)/8}] = \frac{1}{8} [E_{\text{total}}(Ba_4Sr_4Ti_8O_{24-x}) - 4E_{\text{iso}}(Ba) - 4E_{\text{iso}}(Sr) - 8E_{\text{iso}}(Ti) - (24-x)E_{\text{iso}}(O)] \quad (1)$$

The electron density structure of the BST and BST-O on (001) plane are showed in Fig. 2. As is known to all, BST has the perovskite structure and the oxygen octahedron, in which the electrons and all the atoms are achieved Coulomb balance in the pure BST. The Coulomb balance is wrecked when O vacancy appears in BST, all atoms and electrons achieved a new balance point by changing position. In order to keep Coulomb balance when an O atom is removed away, the nearest Ti atoms will move away from the vacancy and be closer to the other O atoms by the action of Coulomb force. Meanwhile, the nearest O atoms will happen relative displacements. These changes will also affect electron cloud configuration of the other atoms. The results can prove that the basic oxygen octahedrons have a notable distortion when an O atom is removed and the distortion will influence the physical properties of the BST importantly.

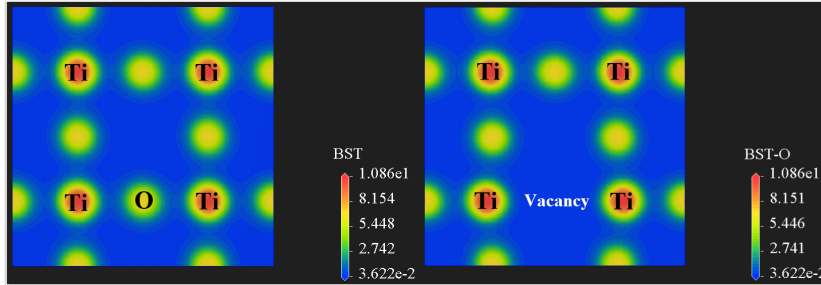


Fig. 2 Electron density map of pure BST and BST with oxygen vacancy in (001) plane

Optical properties of the BST-O

As we know, the optical properties of the dielectric can be well described by complex dielectric function which is expressed as Eq. (2).

$$\varepsilon(\omega) = \varepsilon_1(\omega) + j\varepsilon_2(\omega) \quad (2)$$

Assuming that the light polarization is parallel to the optical axis, the expressions for reflectivity $R(\omega)$, refractive index $n(\omega)$, extinction coefficient $k(\omega)$, optical conductivity $\sigma(\omega) = \sigma_1(\omega) + j\sigma_2(\omega)$, absorption coefficient $I(\omega)$ and energy loss function $L(\omega)$ can be obtained with the dielectric function,

$$R(\omega) = \left| \frac{\sqrt{\varepsilon(\omega)} - 1}{\sqrt{\varepsilon(\omega)} + 1} \right|^2 = \frac{(n-1)^2 + k^2}{(n+1)^2 + k^2} \quad (3)$$

$$n(\omega) = \frac{1}{\sqrt{2}} \left[\sqrt{\varepsilon_1^2(\omega) + \varepsilon_2^2(\omega)} + \varepsilon_1(\omega) \right]^{1/2} \quad (4)$$

$$k(\omega) = \frac{1}{\sqrt{2}} \left[\sqrt{\varepsilon_1^2(\omega) + \varepsilon_2^2(\omega)} - \varepsilon_1(\omega) \right]^{1/2} \quad (5)$$

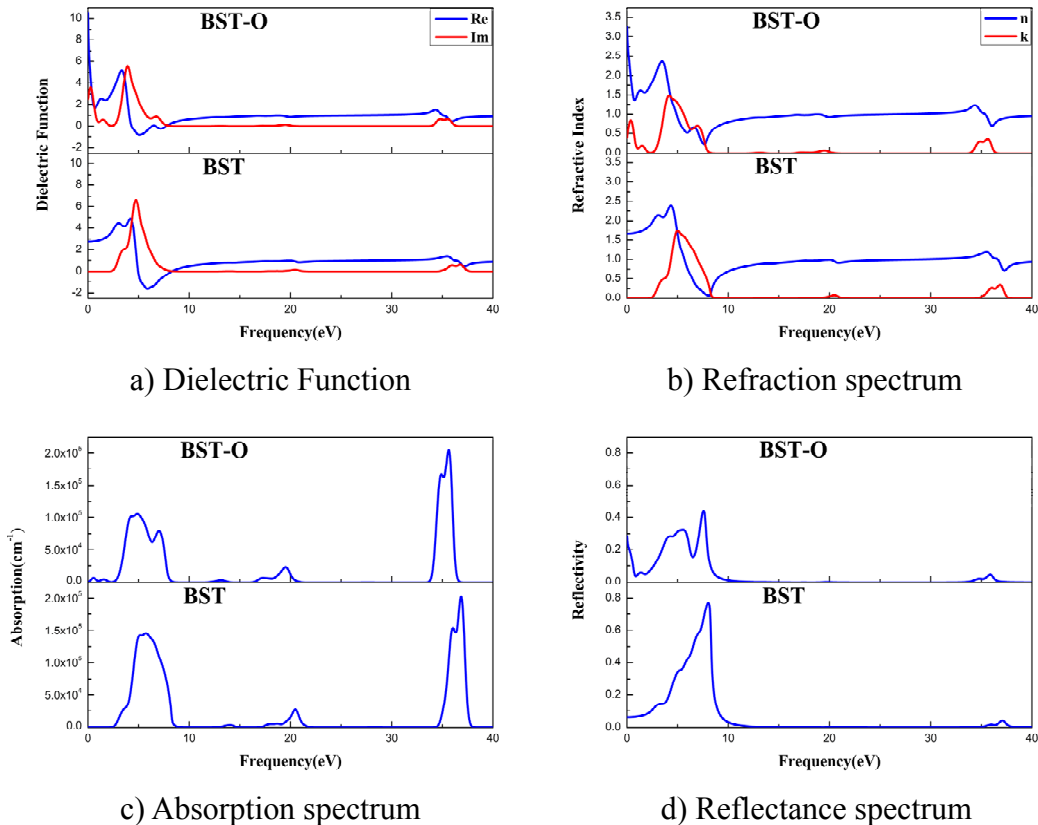
$$\sigma_1(\omega) = \frac{\omega}{4\pi} \varepsilon_2(\omega) \quad (6)$$

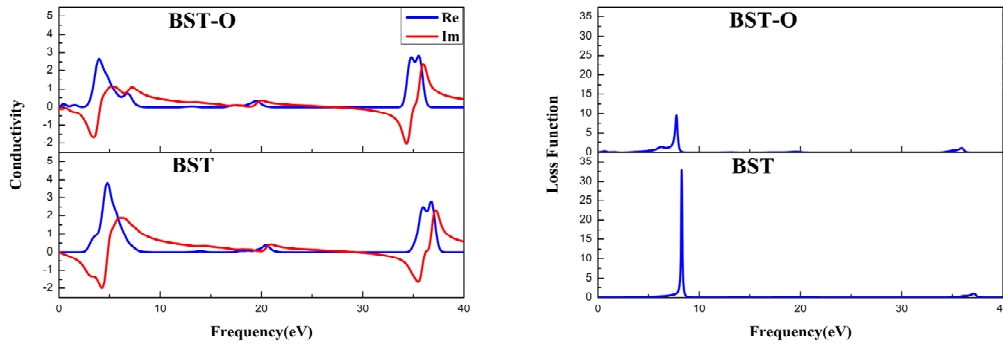
$$\sigma_2(\omega) = -\frac{\omega}{4\pi} [\varepsilon_1(\omega) - 1] \quad (7)$$

$$I(\omega) = \frac{\sqrt{2}\omega}{c} \left[\sqrt{\varepsilon_1^2(\omega) + \varepsilon_2^2(\omega)} - \varepsilon_1(\omega) \right]^{1/2} \quad (8)$$

$$L(\omega) = \text{Im} \left(\frac{-1}{\varepsilon(\omega)} \right) = \frac{\varepsilon_2(\omega)}{\varepsilon_1^2(\omega) + \varepsilon_2^2(\omega)} \quad (9)$$

The optical properties of ordering along a axis were calculated. The comparisons of the calculated optical properties for the pure BST and the BST with O vacancy are shown in Fig. 3. Since the optical performances are the behavior of the response of the dielectric properties in the optical frequency range, the dielectric function of BST and BST-O are plotted in Fig. 3 a), in which the real part of dielectric function $\varepsilon_1(\omega)$ and the imaginary part of dielectric function $\varepsilon_2(\omega)$ were marked by blue line and red line, respectively. In Fig. 3, there is a considerable difference between our calculation data and experiment value (10^4) about dielectric constant. There are two possible reasons for the deviation. Firstly, the local density approximation will underestimate the band gap of insulator or semiconductor. Secondly, the origin of the high dielectric constant of the BST is directly related to its micro and mesoscopic structure, such as grain size, the length of domain wall or the number of dipole under different experiment condition^[14, 20]. When an O defect was introduced in the BST, the results show that the real and imaginary part of dielectric function of BST were far less than that of the BST-O under low frequency, which is consistent with the previous experimental regularity^[21]. In the zero frequency limit, $\varepsilon_1(\mathbf{0})$ is the static dielectric constant, for BST and BST-O the calculated $\varepsilon_1(\mathbf{0})$ are 2.76 eV and 10.48 eV respectively. $\varepsilon_2(\omega)$ spectrum of BST has one prominent peak which is located at 4.73 eV, whereas $\varepsilon_2(\omega)$ of BST-O has two prominent peaks which are located at 0.25 and 3.90 eV.





e) Optical conductivity

f) Energy loss function

Fig. 3 The optical properties of BST with oxygen vacancy and pure BST: a) dielectric function, b) refraction spectrum, c) absorption spectrum, d) reflectance spectrum, e) optical conductivity, f) energy loss function

In order to further study the effect of oxygen vacancy defect on the optical properties of BST, the refractive index $n(\omega)$ and the extinction coefficient $k(\omega)$ are plotted in Fig. 3 b). For $n(\omega)$ of the pure BST, there are two peaks at 3.12 and 4.34 eV and rather steep decrease between 4.37 and 8.09eV, and minimum value is located at 8.09eV, the value of $n(\omega)$ increase continuously toward the first peak from 0 to 3.12 eV, the trend was in accordance with experiment^[22]. With removing an O atom, the main difference between the pure BST and BST-O happened range from 0 to 8.09 eV, the two anomalous dispersion zone appear in visible light frequency region (1.59~3.11 eV) and the value of $n(\omega)$ of the BST-O is higher than that of the BST under low frequency. In comparison with Fig. 3 a), we found the change trend of refractive index $n(\omega)$ and extinction coefficient $k(\omega)$ were in a similar trend with the real part and imaginary part of dielectric function.

Fig. 3 c) shows the absorption spectra of the BST and BST-O. Without exception, the two models possess three major absorption areas: (1) 2.5~8.9 eV, (2) 16.5~21.5 eV, (3) 33.3~38.5 eV, respectively. The three major absorption areas of the BST-O have a slight red shift. From 0 to 2.3 eV, there are two small absorption zones for the BST-O, the reason for this phenomenon perhaps is appearance of anomalous dispersion zone in this range. In (1) zone, the absorption value of the BST-O is much lower than that of pure BST and there are two prominent absorption peaks(4.87 eV, 7.00 eV) for BST-O, whereas absorption spectra of the BST have only one peak(5.71 eV). In (2) and (3) zone, the absorption spectra for BST-O are similar to that of pure BST, but the positions of the peaks of the absorption spectra happened a red shift relative to the pure BST.

The phenomenon that the absorption spectra of the BST-O have multimodality and smaller amplitude also appear in the reflectance spectrum and optical conductivity of the BST-O. Fig. 3 d) and Fig. 3 e) give the reflectance spectrum and the optical conductivity of the BST and BST-O, respectively. In Fig. 3 f), the energy loss function $L(\omega)$ is calculated, which is an important optical parameter describing the energy loss of a fast electron traversing in a BST solid solution. The peak in the $L(\omega)$ spectra represents the plasma resonance and corresponds to the trailing edges in the $R(\omega)$ spectra. Due to the excitation of plasma, $L(\omega)$ shows intense maxima for the BST and BST-O at 8.26 eV and 7.79 eV, which correspond to the abrupt reduction in the $R(\omega)$ spectra.

To give an overview of the optical properties of the BST-O, the calculated optical properties ordered along different directions (a axis, b axis, c axis) were displayed in Fig. 4. When direction of polarization was set along b and c axis, the general trend of optical properties for b axis was same as that of c axis, but there is a big difference between optical properties of a axis and two other directions, which mainly perform different optical properties from 0 to 8.09 eV. In above mentioned regions, the comparison of the dielectric function, refraction spectrum, absorption spectrum, reflectance spectrum, optical conductivity of a axis and two other directions indicates the former have extraordinary multimodality, from Fig. 4 f), the energy loss function $L(\omega)$ of a axis happened a blue shift relative to that of b and c axis and a small peak located at 6.24 eV. Due to O element of

perovskite O octahedron structure playing a important role on the optical properties, the BST-O's optical properties have some differences in different directions, which is called as optical anisotropism^[23]. These results illustrate O vacancy lead to large change on the geometry structure, electronic cloud distribution of BST, which are caused by optical anisotropism.

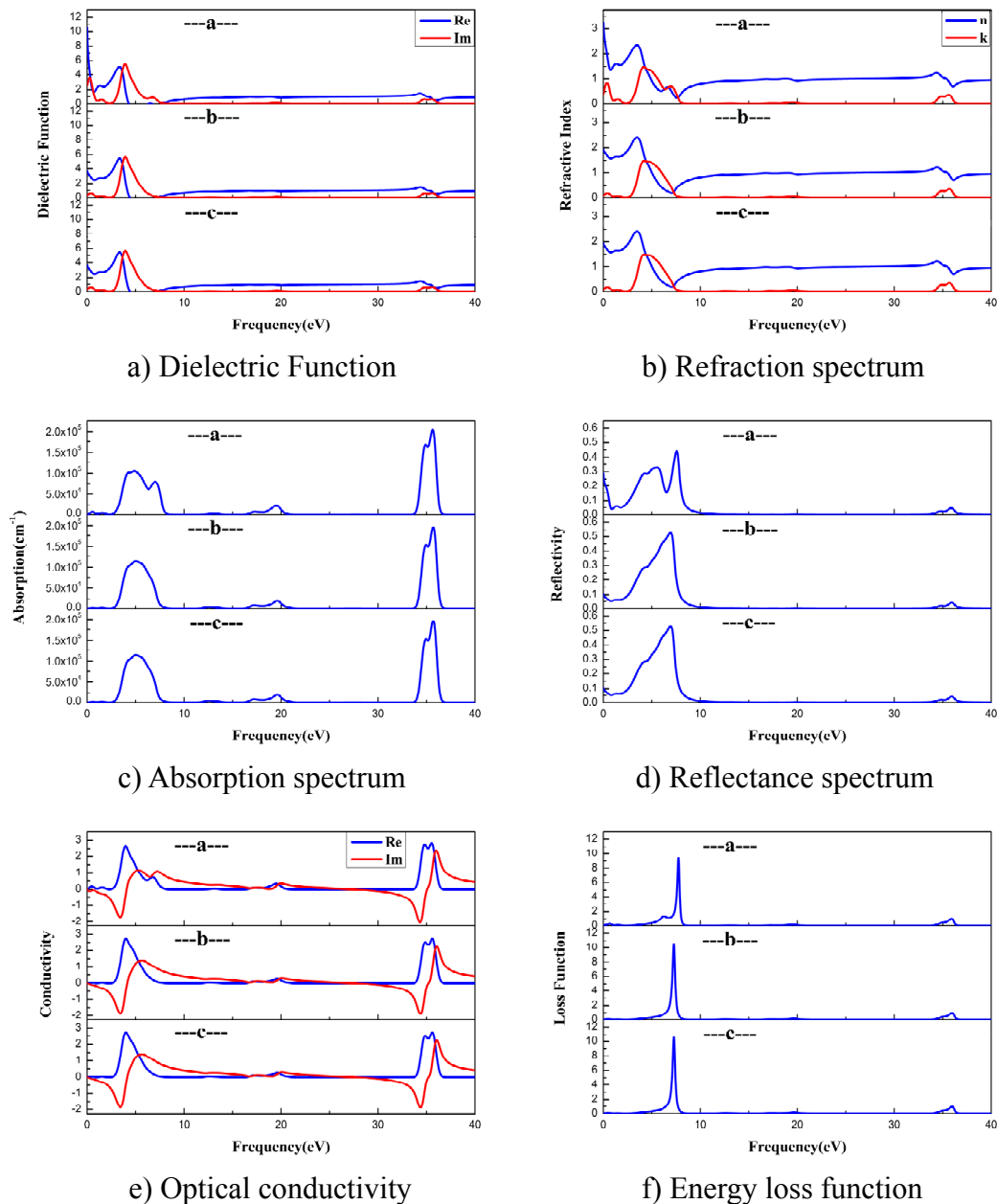


Fig. 4 The optical properties of BST with oxygen vacancy on the a, b and c axis: a) dielectric function, b) refraction spectrum, c) absorption spectrum, d) reflectance spectrum, e) optical conductivity, f) energy loss function

Conclusions

In this work, the effects of O vacancy on geometry structures, electron density distribution and optical properties of the lead-free $Ba_{0.5}Sr_{0.5}TiO_3$ have been investigated using the first principles calculations. Two models of the pure BST and BST with O vacancy were presented. In the case of introducing an O vacancy, the geometry structure of BST has a distortion process relative to the pure BST, which has an important influence on the electron density distribution of the whole cell. By analyzing the optical properties of BST and BST-O, the oxygen vacancies have a key effect on the oxygen octahedron TiO_6 and optical properties; in comparison with the pure BST, the oxygen vacancy lead the increase of refractive index and the decrease of absorption coefficient in visible

light frequency region (1.59~3.11 eV), the optical anisotropism is also found in the BST with O vacancy.

Acknowledgments

This work was supported by the Scientific Research Fund of Heilongjiang Provincial Education Department (No.12531143).

References

- [1] K Su, N Nuraje and N L Yang: *Langmuir* Vol. 23(2007), p. 11369
- [2] S Mornet, C Elissalde, V Hornebecq, et al: *Chem. Mater* Vol. 17(2005), p. 4530
- [3] J Xu, J Zhai and X Yao: *Cryst Growth Des* Vol. 6(2006), p. 2197
- [4] E P Gorzkowski, M J Pan, B Bender, et al: *J. Electroceram* Vol. 18(2007), p. 269
- [5] S Tappe, U Bottger and R Waser: *Appl. Phys. Lett* Vol. 85(2004), p. 624
- [6] T Hu, J Juuti, H Jantunen, et al: *J. Eur. Ceram. Soc* Vol. 27(2007), p. 3997
- [7] P Bao, T J Jackson, X Wang, et al: *J. Phys. D: Appl. Phys* Vol. 41(2008), p. 063001
- [8] R E Cohen: *Nature* Vol. 358(1992), p. 136
- [9] S Hong-Guo, Z Zhong-Xiang, Y Cheng-Xun, et al: *Chin. Phys. Lett* Vol. 29(2012), p. 017303
- [10] N Sai, D Vanderbilt: *Phys. Rev. B* Vol. 62(2000), p. 13942
- [11] J Weerasinghe, D Wang and L Bellaiche: *Phys. Rev. B* Vol. 85(2012), p. 014301
- [12] W D Xue, Y R Li and Y Chun: *J. Chem. Phys* Vol. 18(2005), p. 179
- [13] Y X Wang: *Solid. State. Commun* Vol. 135(2005), p. 290
- [14] F M Pontes, E R Leite, E Longo, et al: *Appl. Phys. Lett* Vol. 76(2000), p. 2433
- [15] S J Clark, M D Segall, C J Pickard, et al: *Z. Kristallogr* Vol. 220(2005), p. 567
- [16] E Cockayne, B P Burton: *Phys. Rev. B* Vol. 62(2000), p. 3735
- [17] J Ding, L W Wen, X B Kang, et al: *Comp. Mater. Sci* Vol. 96(2015), p. 219
- [18] S. Y Kuo, W. Y Liao and W. F Hsieh: *Phys. Rev. B* Vol. 64 (2001), p. 224103
- [19] J Saal, J Andelm, W D Nothwang, et al: *Integr. Ferroelectr* Vol. 101(2008), p. 142
- [20] V R Mudinepalli, L Feng, W C Lin, et al: *J. Adv. Ceram* Vol. 4(2015), p. 46
- [21] G X Dong, W Liu: *Adv. Mater. Res* Vol. 295(2011), p. 1059
- [22] H Y Tian, W G Luo, X H Pu, et al: *J. Phys-Condens. Mat* Vol. 13(2001), p. 4065
- [23] M DrDomenico Jr, S H Wemple: *J. Appl. Phys* Vol. 40(1969), p. 720